

Optical phase encoding in pulsed approach to reservoir computing

Johan Henaff,¹ Matthieu Ansquer,^{1,2} Miguel C Soriano,³ Roberta Zambrini,³ Nicolas Treps,¹ and Valentina Parigi¹

¹Laboratoire Kastler Brossel, Sorbonne Université, ENS-Université PSL,
CNRS, Collège de France, 4 place Jussieu, 75252 Paris, France

²Phasics SA, Batiment Mercury I, Espace technologique,
Route de l'Orme des Merisiers, 91190 Saint-Aubin, France

³Instituto de Física Interdisciplinar y Sistemas Complejos IFISC (CSIC-UIB),
Campus Universitat Illes Balears, E-07122 Palma de Mallorca, Spain

(Dated: January 26, 2024)

The exploitation of the full structure of multimode light fields enables compelling capabilities in many fields including classical and quantum information science. We exploit data-encoding on the optical phase of the pulses of a femtosecond laser source for a photonic implementation of a reservoir computing protocol. Rather than intensity detection, data-reading is done via homodyne detection that accesses combinations of amplitude and phase of the field. Numerical and experimental results on NARMA tasks and laser dynamic predictions are shown. We discuss perspectives for quantum enhanced protocols.

Reservoir computing is a supervised machine learning approach to time series processing, rooted in recurrent neural networks [1, 2]. Inspired by the brain mechanisms, many interconnected artificial neurons process input information and display an internal memory. Recurrent neural networks are then suitable for temporal tasks such as speech recognition [3, 4], but at the expense of being hard to train. All the weights of the networks need indeed to be trained using backpropagation through time [5], a time-consuming and not always converging, procedure [6]. Differently, in the reservoir computing (RC) approach only the weights of the output layer are trained to process information [7, 8]. Those architectures are composed of three elements: an input layer to inject the data into the system, a reservoir composed of a large number of neurons (or nodes) randomly connected, and an output (or reading) layer to extract the information from the reservoir. Under certain conditions on the reservoir, training the output layer with a simple linear regression can be sufficient [1, 8].

In this paper, we present the design of a reservoir computing protocol using a single non linear node with delayed feedback as in [9]. While recent works have successfully implemented reservoir and neuromorphic computing via the frequency components of optical frequency combs [10–12], here we exploit the time features, i.e. the pulses basis, of an optical frequency comb as nodes of the reservoir. Moreover coherent homodyne detection is used, so that information can be encoded in the phase components of the field rather than its intensity or amplitude. We show that despite a small number of nodes and a low non-linearity, our protocol has good performances, displaying both nonlinear memory and forecasting capabilities. Our system builds on the notion that optical pulses can be used to build spiking reservoirs [13, 14] and that phase encoding for information injection can yield to better performance in photonic reservoir computers [15, 16].

Optical based computing [17] might be able to give speed or energy-efficiency benefits over electronics.

Among the peculiar features of optical systems for computing, time and frequency multiplexing can be exploited in our system. In addition, the large signal-to-noise ratio characteristics of the detection pave the way for quantum protocols [18] by exploring quantum features of the optical states. Recently demonstrated frequency and time-multiplexed quantum platforms [19, 20] can then be exploited in promising protocols [21, 22].

In a delayed feedback RC architecture, the reservoir is composed of virtual neurons distributed in time in a feedback loop [9] and only one neuron is accessible at a time. Each neuron is separated from the others by a time interval θ . In the following, we consider V neurons labeled by j . The time-span of the reservoir, τ , is equivalent to its size. It is given by $\tau = V\theta$.

To process a time sequence $u(t)$, the signal is sampled according to $u_k = u(t = kT_s)$, where T_s is the sampling time and $k \in [1 : L]$, with L the length of the input sequence. Each data point u_k is distributed on every node in the time-span of the reservoir. As illustrated in Fig. 1 (input layer), this is achieved by applying a mask function $m(t_j)$ to u_k . This mask is composed of V individual steps of duration θ so that $m_j = m(t_j = j\theta)$ [23].

The state of neuron $r_{j,k}$, corresponding to the j^{th} node for the data point k , at time $t_j = k\tau + j\theta$, is given by a non-linear function of the sum of input data and the previous state of the reservoir $r_{j,k-1}$. The specific description of our reservoir system is detailed later in Eq. 4.

The state of the reservoir is extracted at the output layer y_k , given by a simple linear combination of the reservoir neuron values:

$$y_k = \mathbf{W}_{out}^T \mathbf{r}_k, \quad (1)$$

where \mathbf{r}_k is the vector of V neurons (measured signals), \mathbf{W}_{out} is the vector containing the output weights, and T stands for the transposition of the vector column.

To perform the supervised training, a set of data of length L_{train} is taken. The reservoir states \mathbf{r}_k and the target data \hat{y}_k for the full set of training data are re-

grouped in the vectors $R = (\mathbf{r}_1, \dots, \mathbf{r}_{L_{train}})$ and $\hat{\mathbf{Y}}^T = (\hat{y}_1, \dots, \hat{y}_{L_{train}})$. The training procedure is then reduced to the inversion of a matrix so that \mathbf{W}_{out}^* , the trained set of output weights, is given by $\mathbf{W}_{out}^* = \hat{\mathbf{Y}}R^{-1}$. Note that in practice more complex transformations are used, such as Ridge regression [1], to prevent the protocol from overfitting. The accuracy of the training is assessed on a new set of data, called test-set, of length L_{test} . It is given by computing an error function such as the normalized root mean squared error, or a correlation coefficient such as Pearson coefficient.

As previously mentioned, in this work, the reservoir is composed of a succession of laser pulses. The information is encoded in the phase of each pulse and extracted using homodyne detection. In the following, we derive the expressions corresponding to the experimental configuration presented in Fig. 1.

To describe the experiment, let us start with the expression of the electric field of one pulse given by $E_{pulse}^{(+)}(t) = \mathcal{E}_0 a(t)e^{-i\omega_0 t}$. Even though a high bandwidth detector is used to measure the field pulse by pulse, this detector is not fast enough to resolve the pulse shape. In addition, one data point is taken for each pulse. Thus, we consider that each pulse has some average amplitude a . The information, i.e the input data, can be encoded in the two degrees of freedom of the pulses, their amplitude or their phase. In [21], Nokkala et. al. investigated several RC protocol architectures with different encoding for the input data. In particular, encodings into the amplitude or the phase of a coherent state were compared. They demonstrated numerically that phase encoding can lead to better performance. Therefore, using the fact that under certain conditions the laser field can be assimilated to a coherent state, we choose to encode the information in the phase of the pulses. Hence, the field of the j^{th} pulse at the time step k is multiplied by a phase term containing the injected data at step k and the measurement done at step $k - 1$ according to

$$E_{j,k}^{(+)} = \mathcal{E}_0 a \exp [i(\beta m_j u_k + \alpha M_{k-1,j})], \quad (2)$$

where $E_{j,k}^{(+)}$ is the complex field amplitude of the pulse at time $t_n = k\tau + j\theta$. As shown in the experimental scheme in Fig. 1, data $m_j u_k$ are summed to homodyne measurements $M_{k-1,j}$ at step $k - 1$ via a mixer, in order to provide memory to the system. The gain parameters α and β are set by electronic transfer functions and can be used to optimize the protocol. The homodyne detection measurement $M_{k,j}$ of the node j at time step k , providing the necessary non-linearity for the protocol to work, is then given by:

$$M_{k,j} = C \sin(\beta m_j u_k + \alpha M_{k-1,j}), \quad (3)$$

where C is a constant depending on the detector characteristics and the experimental conditions.

In order to create links between the virtual nodes of the reservoir, we use the finite bandwidth of the system. As

it will be detailed later, the homodyne detector has a response time that is a bit slower than the pulse repetition rate corresponding to the node separation ($\theta = T_r \simeq 6.4$ ns). The bandwidth of the detection determines the parameter T_{BW} of the protocol. In addition, low-pass filters can be added after the detector to reduce even more the effective bandwidth T_{BW} and tune the parameter T_r/T_{BW} . This ratio determines the corresponding graph connectivity of the reservoir [24]. Consequently, the measurement of the node j at time step k is given by

$$\begin{cases} M_{k,j} \simeq C \sin(\phi_{k,j-1})e^{-T_r/T_{BW}} \\ \quad + C \sin(\phi_{k,j})(1 - e^{-T_r/T_{BW}}) \\ \phi_{k,j} = \beta m_j u_k + \alpha M_{k-1,j} \end{cases} \quad (4)$$

From equation (4), we see that each node is connected to a few previous nodes with different strengths. Those connections depend on the ratio T_r/T_{BW} . Changing this ratio modifies the influence of a given node on the future ones.

The scheme of the experimental setup is further illustrated in Fig. 1. As usual in homodyne detection, the field from the laser is split into two, a weak beam, the signal, and a strong beam, the local oscillator (LO). The phase encoding is achieved using an electro-optic modulator (EOM) on the signal arm. By applying a voltage to this modulator, the phase of each pulse can be modified to encode the information. This EOM is driven from a computer via an arbitrary waveform generator (AWG). For simplicity, we decided to implement the feedback electronically as in [9] and not optically as in [25]. An optical feedback would require an optical loop. Such loops are usually built using fiber elements, which are not easy to handle with femtosecond pulses, mainly due to chromatic dispersion. As long delays are difficult to handle in free space, we have chosen the electronic feedback. This is achieved by first detecting the electric field after the encoding via an homodyne detection, which is equivalent to measuring the nodes of the reservoir. The detection is performed by a home-made high-bandwidth balanced detector. Its bandwidth is approximately 100 MHz and details about this detector can be found in [26]. To create the links between the nodes, a low pass filter is introduced after the detection ($T_{BW} \simeq 21ns$). After detection, the measured signal is split in two. A small part is gathered for off-line processing and the other part is sent in a long coaxial cable to create the feedback loop that provides the reservoir memory. The delayed signal is finally mixed with the input signal from the AWG to be sent to the EOM, creating the feedback loop. At the time of the experiment, the longest cable in the lab with sufficiently low losses could only handle a delay corresponding to $V=35$ nodes thus defining the size and corresponding maximum memory available to the RC system.

To characterize the computing abilities of the setup, we first report the results for an academic benchmark, namely the NARMA (Nonlinear AutoRegressive Moving Average) task. It involves predicting the next output

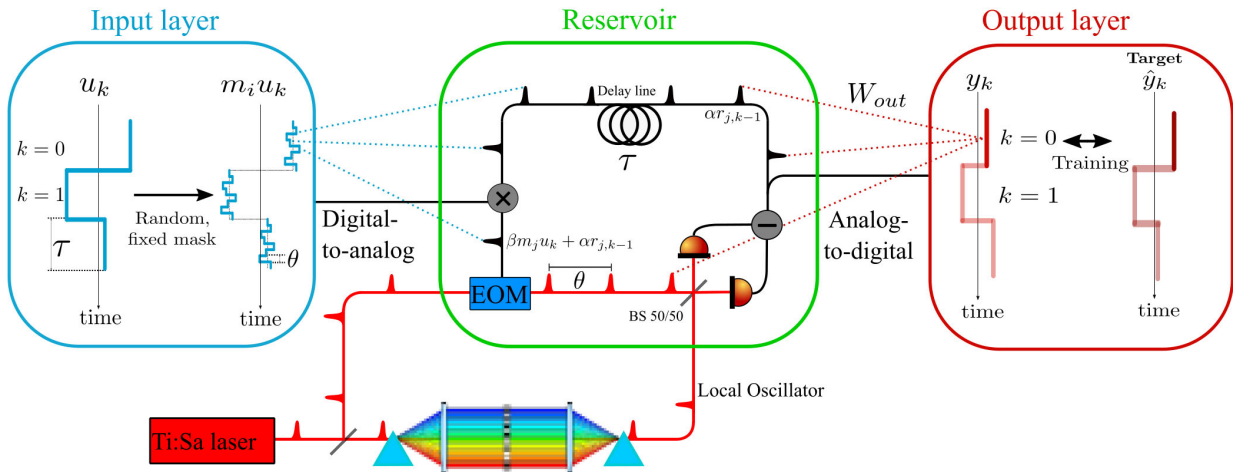


Figure 1. **Experimental scheme of the delay-based reservoir computing architecture.** The optical field generated by a Ti:Sa laser is separated in two. The weak beam, the signal, is sent into an electro-optic modulator (EOM) controlled by an arbitrary waveform generator (AWG). Information is encoded in the phase of each pulse by applying a voltage to the EOM. The strong beam, the local oscillator, is sent into a pulse shaper to match the dispersion introduced by the EOM on the other arm. Both beams are combined on a 50-50 beam-splitter and detected by a high bandwidth balanced detector. After low pass filtering, to control the parameter T_{BW} , the signal is sent into a long coaxial cable to create a delay. A part of this signal is then mixed with the input data to create the feedback. The other part of the signal is acquired to proceed to the off-line training of the output weights. Optical and electronic pulses are represented in red and black, respectively.

value in a sequence based on a non-linear combination of past output values and input data. It is defined by [27, 28]

$$y(t) = 0.3y(t-1) + 0.05y(t-1) \sum_{i=t-N}^t y(i) + 1.5u(t-1)u(t-N) + 0.1, \quad (5)$$

where the input u is taken from a uniform random distribution in the interval $[0, 0.5]$. The parameter N determines how many time steps in the past of inputs in u influence the current output y . The drawn sequence u is used as the input to our reservoir, which is then trained on the corresponding target output y . The performance of the protocol is evaluated by the Pearson correlation coefficient between the NARMA- N value y and the predicted value \hat{y} .

As shown in Fig. 2, for a small value of input delay parameter ($N = 2$) the experimental RC protocol can approximate the target data. The accuracy of the approximation decreases monotonically for higher values of N as shown in Fig. 3 (solid line). In addition to the optical experimental protocol, we performed numerical simulations. They are run according to Eq. (4), given the known characteristics of the experiment (e.g. detection noise, sampling rate in acquisition). We find that the performances of the experimental setup are qualitatively similar to the simulated ones, see dashed black line in Fig. 3. The discrepancies between experiment and simulation may be due to the presence of other experimental noise sources, such as phase drifts, not accounted for in the

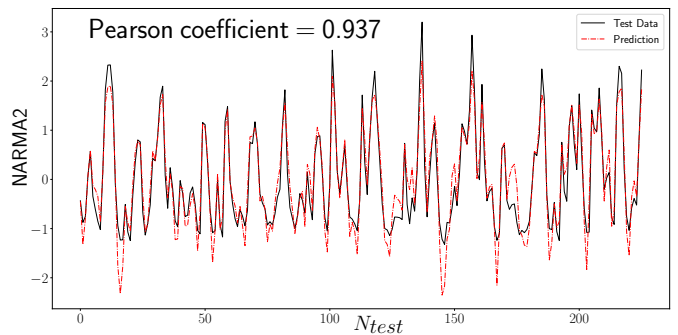


Figure 2. **Experimental prediction of NARMA-2 function.** The protocol was trained on 2250 input data and tested on 600.

numerical simulations. It is also worth mentioning that the α and β parameters can be finely tuned in the simulation while in the experiment the α parameter was set with an electronic attenuator that didn't allow fine tuning, therefore we couldn't reach identical (α, β) . Even though a quantitative agreement is not possible, the numerical simulations allows us to estimate the impact of an increasing reservoir size. The red line in Fig. 3 indicates that the error in the NARMA- N task is greatly reduced when the number of nodes is increased to 100. Similar trends can be expected to happen if the reservoir size could be increased in the experimental implementation.

To give an example of a practical application of this machine learning protocol, following the idea of [29, 30], we aim to predict the dynamics of the fluctuations of the laser studied in [31]. It was demonstrated that the

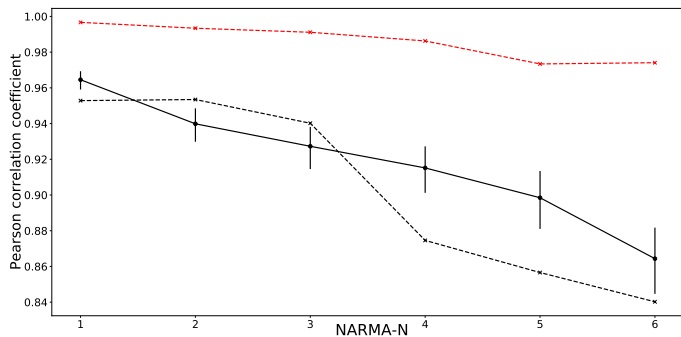


Figure 3. **Pearson correlation coefficient as a function of the input delay parameter N .** Experiment (solid line) and simulation (dashed line) were trained on 2250 input data and tested on 600. Black lines correspond to the experimental and numerical results for 35 virtual nodes. Increasing the number of nodes to 100 (red) reduces the error. The simulations have been performed for $\alpha = 0.7$ and $\beta = 1.0$.

amplitude and phase noises are mainly induced by the pump laser intensity noise. Consequently, in this section, we try to predict the power $\delta\epsilon$ and central frequency $\delta\omega_c$ fluctuations from the intensity noise of the pump laser.

As we aim to predict the intensity related dynamics, the intensity fluctuations of the pump power are used as input data. They are measured with a photodiode from a leak in the laser cavity. The output data, used as target, are the fluctuations of each laser variable, measured using the experimental scheme described in [31]. Those quantities are recorded simultaneously. Each acquisition is composed of 10000 data points. We take 8000 data points to train the reservoir. The 2000 remaining points are used as a validation set to see how well the algorithm performs.

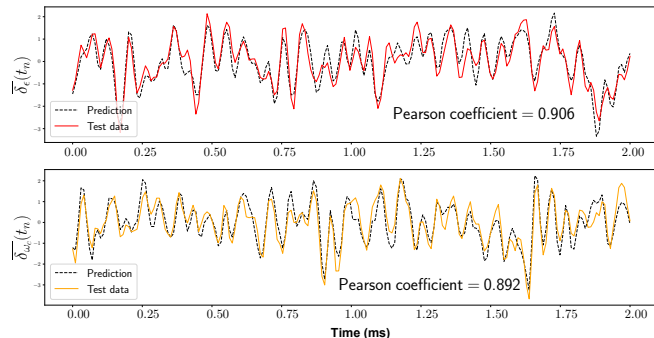


Figure 4. **Performance of the protocol on laser dynamics prediction.** The input data used for the training are the fluctuations of the pump laser power. The laser power fluctuation is in red and the central frequency fluctuation in yellow.

The mean power noise and the center spectrum, predicted after training from the pump laser fluctuations to

gether with the expected signal are presented on Fig. 4. It can be seen that the experimental prediction is close to the real measured noise in both cases. Given these positive results, one could think of an active stabilization of the laser using the reservoir computing approach combined with a feedback control loop.

In conclusion we implemented an optical reservoir computing protocol exploiting the pulse basis of an optical frequency comb. The use of a homodyne detection for readout allowed us to encode the information in the phase of the coherent states. This experimental proof-of concept has a relatively small number of virtual nodes and a single hardware node that operates in a low nonlinearity regime, yet is proven to perform non-trivial computational tasks. This work paves the way toward more refined protocol with an all-optical configuration.

Moreover, recent work in the squeezing generation at high repetition rate [19] could be used to implement a quantum reservoir computing protocol with a scheme similar to the one of this article. The use of quantum states and the spectral multimode nature of our frequency comb could be harnessed to improve the computational capacity of our protocol as suggested in [22].

Funding

European Research Council under the Consolidator Grant COQCOoN (Grant No. 820079) and the Agence Nationale de la Recherche with support of the Direction Générale de l’Armement (LASAGNE ANR-16-ASTR-0010-03). We acknowledge the Spanish State Research Agency, through the María de Maeztu project CEX2021-001164-M funded by the MCIN/AEI/10.13039/501100011033 and through the COQUSY project PID2022-140506NB-C21 funded by MCIN/AEI/10.13039/501100011033, MINECO through the QUANTUM SPAIN project, and EU through the RTRP - NextGenerationEU within the framework of the Digital Spain 2025 Agenda.

Disclosures

The authors declare no conflicts of interest.

Data availability

Data underlying the results presented in this paper are not publicly available at this time but may be obtained from the authors upon reasonable request.

-
- [1] M. Lukoševičius and H. Jaeger, Reservoir computing approaches to recurrent neural network training, *Computer science review* **3**, 127 (2009).
- [2] K. Nakajima and I. Fischer, *Reservoir computing: Theory, physical implementations, and applications* (Springer, 2021).
- [3] D. Verstraeten, B. Schrauwen, and D. Stroobandt, Reservoir-based techniques for speech recognition, in *The 2006 IEEE International Joint Conference on Neural Network Proceedings* (IEEE, 2006) pp. 1050–1053.
- [4] L. Larger, A. Baylón-Fuentes, R. Martinenghi, V. S. Udaltsov, Y. K. Chembo, and M. Jacquot, High-Speed Photonic Reservoir Computing Using a Time-Delay-Based Architecture: Million Words per Second Classification, *Physical Review X* **7**, 011015 (2017).
- [5] P. J. Werbos, Backpropagation through time: what it does and how to do it, *Proceedings of the IEEE* **78**, 1550 (1990).
- [6] K. Doya *et al.*, Bifurcations in the learning of recurrent neural networks 3, *learning (RTRL)* **3**, 17 (1992).
- [7] H. Jaeger, Harnessing Nonlinearity: Predicting Chaotic Systems and Saving Energy in Wireless Communication, *Science* **304**, 78 (2004).
- [8] H. Jaeger, The “echo state” approach to analysing and training recurrent neural networks—with an erratum note, Bonn, Germany: German National Research Center for Information Technology GMD Technical Report **148**, 13 (2001).
- [9] L. Appeltant, M. Soriano, G. Van der Sande, J. Danckaert, S. Massar, J. Dambre, B. Schrauwen, C. Mirasso, and I. Fischer, Information processing using a single dynamical node as complex system, *Nature Communications* **2**, 468 (2011).
- [10] X. Xu, W. Han, M. Tan, Y. Sun, Y. Li, J. Wu, R. Morandotti, A. Mitchell, K. Xu, and D. J. Moss, Neuromorphic computing based on wavelength-division multiplexing, *IEEE Journal of Selected Topics in Quantum Electronics* **29**, 7400112 (2023).
- [11] L. Butschek, A. Akrouf, E. Dimitriadou, A. Lupo, M. Haelterman, and S. Massar, Photonic reservoir computer based on frequency multiplexing, *Opt. Lett.* **47**, 782 (2022).
- [12] A. Lupo, E. Picco, M. Zajmulina, and S. Massar, Deep photonic reservoir computer based on frequency multiplexing with fully analog connection between layers, *Optica* **10**, 1478 (2023).
- [13] D. Owen-Newns, J. Robertson, M. Hejda, and A. Hurtado, Ghz rate neuromorphic photonic spiking neural network with a single vertical-cavity surface-emitting laser (vcSEL), *IEEE Journal of Selected Topics in Quantum Electronics* **29**, 1500110 (2022).
- [14] D. Owen-Newns, J. Robertson, M. Hejda, and A. Hurtado, Photonic spiking neural networks with highly efficient training protocols for ultrafast neuromorphic computing systems, *Intelligent Computing* **2**, 0031 (2023).
- [15] I. Bauwens, K. Harkhoe, P. Bienstman, G. Verschaffelt, and G. V. der Sande, Influence of the input signal’s phase modulation on the performance of optical delay-based reservoir computing using semiconductor lasers, *Opt. Express* **30**, 13434 (2022).
- [16] K. Kanno, A. A. Haya, and A. Uchida, Reservoir computing based on an external-cavity semiconductor laser with optical feedback modulation, *Optics Express* **30**, 34218 (2022).
- [17] P. L. McMahon, The physics of optical computing, *Nature Reviews Physics* **5**, 717 (2023).
- [18] P. Mujal, R. Martínez-Peña, J. Nokkala, J. García-Beni, G. L. Giorgi, M. C. Soriano, and R. Zambrini, Opportunities in quantum reservoir computing and extreme learning machines, *Advanced Quantum Technologies* **4**, 2100027 (2021).
- [19] T. Kouadou, F. Sansavini, M. Ansquer, J. Henaff, N. Treps, and V. Parigi, Spectrally shaped and pulse-by-pulse multiplexed multimode squeezed states of light, *APL Photonics* **8**, 086113 (2023).
- [20] V. Roman-Rodriguez, D. Fainsin, G. L. Zanin, N. Treps, E. Diamanti, and V. Parigi, Spectrally multimode squeezed states generation at telecom wavelengths (2023), arXiv preprint arXiv:2306.07267.
- [21] J. Nokkala, R. Martínez-Peña, G. L. Giorgi, V. Parigi, M. C. Soriano, and R. Zambrini, Gaussian states of continuous-variable quantum systems provide universal and versatile reservoir computing, *Communications Physics* **4**, 53 (2021).
- [22] J. García-Beni, G. L. Giorgi, M. C. Soriano, and R. Zambrini, Scalable photonic platform for real-time quantum reservoir computing, *Phys. Rev. Appl.* **20**, 014051 (2023).
- [23] S. Ortín, L. Pesquera, G. Van der Sande, and M. C. Soriano, Time delay systems for reservoir computing, in *Photonic Reservoir Computing*, edited by D. Brunner, M. C. Soriano, and G. Van der Sande (De Gruyter, Berlin, Boston, 2019) pp. 117–152.
- [24] D. Brunner, B. Penkovsky, B. A. Marquez, M. Jacquot, I. Fischer, and L. Larger, Tutorial: Photonic neural networks in delay systems, *Journal of Applied Physics* **124** (2018).
- [25] D. Brunner, M. C. Soriano, C. R. Mirasso, and I. Fischer, Parallel photonic information processing at gigabyte per second data rates using transient states, *Nature Communications* **4**, 1364 (2013).
- [26] K. Tiphaine, *Single-Pass Generation and Detection of Ultrafast Multimode Squeezed Light*, Ph.D. thesis, Université Pierre et Marie Curie-Paris VI (2021).
- [27] A. F. Atiya and A. G. Parlos, New results on recurrent network training: unifying the algorithms and accelerating convergence, *IEEE transactions on neural networks* **11**, 697 (2000).
- [28] H. Jaeger, Adaptive nonlinear system identification with echo state networks, *Advances in neural information processing systems* **15**, 609 (2002).
- [29] P. Amil, M. C. Soriano, and C. Masoller, Machine learning algorithms for predicting the amplitude of chaotic laser pulses, *Chaos* **29**, 113111 (2019), arXiv: 1911.04815.
- [30] A. Cunillera, M. C. Soriano, and I. Fischer, Cross-predicting the dynamics of an optically injected single-mode semiconductor laser using reservoir computing, *Chaos* **29**, 113113 (2019).
- [31] M. Ansquer, V. Thiel, S. De, B. Argence, G. Gredat, F. Bretenaker, and N. Treps, Unveiling the dynamics of optical frequency combs from phase-amplitude correlations, *Phys. Rev. Research* **3**, 033092 (2021).

- [32] S. Yokoyama, R. Ukai, S. C. Armstrong, C. Sornphiphatphong, T. Kaji, S. Suzuki, J.-i. Yoshikawa, H. Yonezawa, N. C. Menicucci, and A. Furusawa, Ultra-large-scale continuous-variable cluster states multiplexed in the time domain, *Nature Photonics* **7**, 982 (2013).
- [33] D. Brunner, M. C. Soriano, and G. Van der Sande, *Photonic Reservoir Computing: Optical Recurrent Neural Networks* (Walter de Gruyter GmbH & Co KG, 2019).
- [34] G. Van der Sande, D. Brunner, and M. C. Soriano, Advances in photonic reservoir computing, *Nanophotonics* **6**, 10.1515/nanoph-2016-0132 (2017).
- [35] J. Dong, M. Rafayelyan, F. Krzakala, and S. Gigan, Optical Reservoir Computing using multiple light scattering for chaotic systems prediction, *IEEE Journal of Selected Topics in Quantum Electronics* **26**, 1 (2020), arXiv: 1907.00657.
- [36] F. Duport, B. Schneider, A. Smerieri, M. Haelterman, and S. Massar, All-optical reservoir computing, *Optics Express* **20**, 22783 (2012).
- [37] L. Grigoryeva and J.-P. Ortega, Universal discrete-time reservoir computers with stochastic inputs and linear readouts using non-homogeneous state-affine systems, arXiv:1712.00754 [cs] (2018), arXiv: 1712.00754.
- [38] M. Rafayelyan, J. Dong, Y. Tan, F. Krzakala, and S. Gigan, Large-Scale Optical Reservoir Computing for Spatiotemporal Chaotic Systems Prediction, arXiv:2001.09131 [physics] (2020), arXiv: 2001.09131.
- [39] K. Kanno, A. A. Haya, and A. Uchida, Reservoir computing based on an external-cavity semiconductor laser with optical feedback modulation, *Opt. Express* **30**, 34218 (2022).
- [40] A. Akrouf, A. Bouwens, F. Duport, Q. Vinckier, M. Haelterman, and S. Massar, Parallel photonic reservoir computing using frequency multiplexing of neurons, arXiv:1612.08606 [physics] (2016), arXiv: 1612.08606.
- [41] Q. Vinckier, F. Duport, A. Smerieri, K. Vandoorne, P. Bienstman, M. Haelterman, and S. Massar, High-performance photonic reservoir computer based on a coherently driven passive cavity, *Optica* **2**, 438 (2015).
- [42] Q. Vinckier, F. Duport, M. Haelterman, and S. Massar, Information processing using an autonomous all-photon reservoir computer based on coherently driven passive cavities, in *Frontiers in Optics 2015* (OSA, San Jose, California, 2015) p. FTu3B.6.
- [43] W. Kassa, E. Dimitriadou, M. Haelterman, S. Massar, and E. Bente, Towards integrated parallel photonic reservoir computing based on frequency multiplexing, in *Neuro-inspired Photonic Computing*, edited by M. Sciamanna and P. Bienstman (SPIE, Strasbourg, France, 2018) p. 2.
- [44] A. Smerieri, F. Duport, Y. Paquot, B. Schrauwen, M. Haelterman, and S. Massar, Analog readout for optical reservoir computers, arXiv:1209.3129 [physics] (2012), arXiv: 1209.3129.
- [45] G. Tanaka, T. Yamane, J. B. Héroux, R. Nakane, N. Kanazawa, S. Takeda, H. Numata, D. Nakano, and A. Hirose, Recent advances in physical reservoir computing: A review, *Neural Networks* **115**, 100 (2019).
- [46] J. Pauwels, G. Verschaffelt, S. Massar, and G. Van der Sande, Distributed Kerr Non-linearity in a Coherent All-Optical Fiber-Ring Reservoir Computer, *Frontiers in Physics* **7**, 138 (2019).
- [47] L. Larger, M. C. Soriano, D. Brunner, L. Appeltant, J. M. Gutiérrez, L. Pesquera, C. R. Mirasso, and I. Fischer, Photonic information processing beyond Turing: an optoelectronic implementation of reservoir computing, *Optics Express* **20**, 3241 (2012).
- [48] Y. Paquot, F. Duport, A. Smerieri, J. Dambre, B. Schrauwen, M. Haelterman, and S. Massar, Optoelectronic Reservoir Computing, *Scientific Reports* **2**, 287 (2012).
- [49] X. Xu, M. Tan, B. Corcoran, J. Wu, T. G. Nguyen, A. Boes, S. T. Chu, B. E. Little, R. Morandotti, A. Mitchell, D. G. Hicks, and D. J. Moss, Single photonic perceptron based on a soliton crystal kerr microcomb for high-speed, scalable, optical neural networks (2020), arXiv:2003.01347 [physics.optics].
- [50] J. Dambre, D. Verstraeten, B. Schrauwen, and S. Massar, Information Processing Capacity of Dynamical Systems, *Scientific Reports* **2**, 514 (2012).
- [51] V. Dunjko and P. Wittek, A non-review of Quantum Machine Learning: trends and explorations, *Quantum Views* **4**, 32 (2020), publisher: Verein zur Förderung des Open Access Publizierens in den Quantenwissenschaften.
- [52] M. Schuld, I. Sinayskiy, and F. Petruccione, An introduction to quantum machine learning, *Contemporary Physics* **56**, 172 (2015), arXiv: 1409.3097.
- [53] S. Ortín and L. Pesquera, Tackling the Trade-Off Between Information Processing Capacity and Rate in Delay-Based Reservoir Computers, *Frontiers in Physics* **7**, 210 (2019).
- [54] Z. Lu, J. Pathak, B. Hunt, M. Girvan, R. Brockett, and E. Ott, Reservoir observers: Model-free inference of unmeasured variables in chaotic systems, *Chaos* **27**, 041102 (2017).
- [55] S. Kako, T. Leleu, Y. Inui, F. Khoystatee, S. Reifstein, and Y. Yamamoto, Coherent Ising machines with error correction feedback, *Advanced Quantum Technologies* , 2000045 (2020), arXiv: 2005.10895.
- [56] J. Chen, H. I. Nurdin, and N. Yamamoto, Temporal Information Processing on Noisy Quantum Computers, arXiv:2001.09498 [quant-ph, stat] 10.1103/PhysRevApplied.14.024065 (2020), arXiv: 2001.09498.
- [57] F. Marquardt, *Machine Learning and Quantum Devices*, p. 40.
- [58] H. Jaeger, A tutorial on training recurrent neural networks, covering BPPT, RTRL, EKF and the "echo state network" approach, p. 46.
- [59] J. Dong, R. Ohana, M. Rafayelyan, and F. Krzakala, Reservoir Computing meets Recurrent Kernels and Structured Transforms, arXiv:2006.07310 [cs, eess, stat] (2020), arXiv: 2006.07310.
- [60] A. Goudarzi, P. Banda, M. R. Lakin, C. Teuscher, and D. Stefanovic, A Comparative Study of Reservoir Computing for Temporal Signal Processing, arXiv:1401.2224 [cs] (2014), arXiv: 1401.2224.
- [61] A. Rodan and P. Tiño, Simple Deterministically Constructed Cycle Reservoirs with Regular Jumps, *Neural Computation* **24**, 1822 (2012).
- [62] M. Lukoševičius, A Practical Guide to Applying Echo State Networks, in *Neural Networks: Tricks of the Trade*, Vol. 7700, edited by G. Montavon, G. B. Orr, and K.-R. Müller (Springer Berlin Heidelberg, Berlin, Heidelberg, 2012) pp. 659–686, series Title: Lecture Notes in Computer Science.
- [63] I. B. Yildiz, H. Jaeger, and S. J. Kiebel, Re-visiting the echo state property, *Neural Networks* **35**, 1 (2012).

- [64] C. Gallicchio, A. Micheli, and L. Pedrelli, Deep reservoir computing: A critical experimental analysis, *Neurocomputing* **268**, 87 (2017), advances in artificial neural networks, machine learning and computational intelligence.
- [65] M. Borghi, S. Biasi, and L. Pavesi, Reservoir computing based on a silicon microring and time multiplexing for binary and analog operations, arXiv:2101.01664 [physics] (2021), arXiv: 2101.01664.
- [66] L. C. G. Govia, G. J. Ribeill, G. E. Rowlands, H. K. Krovi, and T. A. Ohki, Quantum reservoir computing with a single nonlinear oscillator, *Physical Review Research* **3**, 013077 (2021).
- [67] Y. Jiang, W. Zhang, F. Yang, and Z. He, Photonic Convolution Neural Network Based on Interleaved Time-Wavelength Modulation, arXiv:2102.09561 [physics] (2021), arXiv: 2102.09561.
- [68] A. E. Hoerl and R. W. Kennard, Ridge regression: applications to nonorthogonal problems, *Technometrics* **12**, 69 (1970).
- [69] J. Aasi, J. Abadie, B. Abbott, R. Abbott, T. Abbott, M. Abernathy, C. Adams, T. Adams, P. Addesso, R. Adhikari, *et al.*, Enhanced sensitivity of the ligo gravitational wave detector by using squeezed states of light, *Nature Photonics* **7**, 613 (2013).
- [70] A. Einstein, B. Podolsky, and N. Rosen, Can quantum-mechanical description of physical reality be considered complete?, *Phys. Rev.* **47**, 777 (1935).
- [71] S. L. Braunstein, Squeezing as an irreducible resource, *Phys. Rev. A* **71**, 055801 (2005).
- [72] V. Roman-Rodriguez, B. Brecht, S. K. C. Silberhorn, N. Treps, E. Diamanti, and V. Parigi, Continuous variable multimode quantum states via symmetric group velocity matching, *New Journal of Physics* **23**, 043012 (2021).
- [73] G. Patera, *Quantum properties of ultra-short pulses generated by SPOPOs: multi-mode squeezing and entanglement*, Ph.D. thesis, Université Pierre et Marie Curie-Paris VI (2008).
- [74] S. Jiang, N. Treps, and C. Fabre, A time/frequency quantum analysis of the light generated by synchronously pumped optical parametric oscillators, *New Journal of Physics* **14**, 043006 (2012).
- [75] T. Michel, *Optimization of the pump spectral shape in a parametric down conversion process to generate multimode entangled states.*, Ph.D. thesis, Research School of Physics, ANU College of Science, The Australian National University (2021).
- [76] G. Patera, N. Treps, C. Fabre, and G. J. De Valcarcel, Quantum theory of synchronously pumped type i optical parametric oscillators: characterization of the squeezed supermodes, *The European Physical Journal D* **56**, 123 (2010).
- [77] R. M. De Araujo, *Génération et manipulation de peignes de fréquences quantiques multimodes*, Ph.D. thesis, Université Pierre et Marie Curie-Paris VI (2012).
- [78] H. Caulfield, J. Kinser, and S. Rogers, Optical neural networks, *Proceedings of the IEEE* **77**, 1573 (1989).
- [79] Y. Zuo, B. Li, Y. Zhao, Y. Jiang, Y.-C. Chen, P. Chen, G.-B. Jo, J. Liu, and S. Du, All-optical neural network with nonlinear activation functions, *Optica* **6**, 1132 (2019).
- [80] V. J. Mathews and J. Lee, Adaptive algorithms for bilinear filtering, in *Advanced Signal Processing: Algorithms, Architectures, and Implementations V*, Vol. 2296, edited by F. T. Luk, International Society for Optics and Photonics (SPIE, 1994) pp. 317 – 327.